MODELLING ISSUES IN SIMULATION OF DEEP EXCAVATIONS

R. Nishanthan, D.S. Liyanapathirana and C.J. Leo
School of Computing, Engineering and Mathematics, University of Western Sydney, Locked Bag 1797, Penrith NSW 2751 Australia.

ABSTRACT

This paper investigates three different modelling approaches available in ABAQUS/Standard finite element program for the simulation of short-term behaviour of deep excavations in saturated clayey soils below the water table. The first approach is based on the total stress principle with the undrained soil properties, which is the conventional way of analysing deep excavations using the finite element method with the undrained assumption. The other two approaches are based on the effective stress principle but the analysis time is very short preventing any excess pore pressure dissipation, replicating undrained behaviour. In the first approach based on the effective stress principle, a partially coupled analysis is carried out considering the excess pore pressures and effective stresses. ABAQUS does not have the ability to incorporate initial hydrostatic pore pressure distribution in the partially coupled excess pore pressure analysis. To simulate the hydrostatic pressures applied on the wall during dewatering of the excavation, body loads are applied along the wall. In the second approach, which resembles the real scenario, a fully coupled analysis was carried out considering the total pore pressures and effective stresses. In this analysis, initial hydrostatic pressures can be established before the excavation begins. Undrained and drained shear strength parameters relevant for the same clayey soil derived from triaxial tests were used to perform the total and effective stress analyses, respectively. Results obtained from a hypothetical case show that the use of the conventional way of analysis based on the total stress principle assuming undrained behaviour is not suitable to predict wall and ground deformations during excavations if the excavation is deep (more than 10 m). Partially-coupled analysis over predicted wall deformations and ground surface settlements compared to the fully coupled analysis, confirming that a fully coupled analysis is necessary to obtain the wall deformation and ground surface settlement corresponding to the short-term behaviour. Finally a case study reported in the literature for a staged deep excavation carried out in Taiwan is simulated using the two methods based on the effective stress principle. These results show that both partially and fully coupled approaches are suitable for the simulation of deep excavations, when excess pore pressure dissipation is allowed during the excavation.

1 INTRODUCTION

Construction activities for high rise buildings tunnels and subway stations are increasing in urban areas to satisfy the demand of ever increasing population. The stress relief during excavations for these construction activities induce ground movements in the vicinity. Since the adjacent service lines and structures are very sensitive to these ground movements, reliable prediction of lateral deformations and ground settlements plays a major role in the design of effective supporting systems to retain the soil around excavations.

Empirical methods and finite element method are used to predict ground movements due to excavations. According to Hsieh and Ou (1998) the finite element method is superior in predicting the wall deformations but alternative empirical methods provide better settlement profiles behind the wall. Although empirical methods are simple and less time consuming compared to a finite element analysis, they do not consider the influence of soil consolidation, construction sequence and stiffness of the support system, when calculating the ground surface settlement and wall deflection. However, a finite element analysis has the ability to simulate all these effects. Finite element method of analysis has been extensively used by many researchers. The majority of these analyses are carried out assuming that the soil is either undrained or fully drained during the excavation.

Ng *et al*. (2004), Finno *et al*. (2007), Yoo and Lee (2008) and Kumar and Chakraborty (2012) carried out finite element analyses assuming fully drained condition. Undrained assumption is valid for simulation of excavations, only if the excavation is rapid and little drainage occurs within the construction duration. Ou *et al*. (1993), Hu *et al*. (2003), Zdravkovic *et al.* (2005), Andresen (2006), Karlsrud and Andresen (2005), Kung *et al.* (2007), Hou *et al*. (2009), Tang and Kung (2010) and Khatri and Kumar (2010) carried out finite element analyses assuming fully undrained behaviour for the soil. Analysing three different cases: (i) undrained inside the excavation and establishing the measured pore pressure distribution behind the wall (ii) undrained both sides of the wall and (iii) undrained inside the excavation and retained soil but allowing a 2.9 m wide region behind the wall to drain. Ng *et al.* (1998) showed that predictions can be improved by taking into consideration drainage due to consolidation. By comparing an undrained and a partially drained analysis, Costa *et al*. (2007) also showed that results from a partially drained analysis incorporating consolidation agree well with the measured data because in reality soil is in a partially drained state during the staged construction procedure. Finno *et al*. (1991), Hsi and Small (1993) and Hashash (1992) utilised partially or fully coupled

finite element procedures to analyse staged constructions. Two major issues ignored in most of the above discussed finite element analysis procedures are: (i) wall installation effects on the subsequent ground and wall deformations due to excavations and (ii) unbalanced forces due to hydrostatic pressure difference acting on the wall due to water pumping out of the excavation to accommodate the construction of floor slabs or temporary support systems for the wall. Simulation of wall installation in a finite element analysis is a challenging task but Finno *et al.* (1991) proposed a method to incorporate wall installation effects into a coupled finite element analysis explicitly.

If a fully coupled finite element analysis based on the effective stress principal is carried out, during the element removal to simulate the excavation, hydrostatic pressure distribution around the wall is automatically adjusted according to the depth of excavation (by lowering the water table within the excavation up to the excavated depth). However, if a fully drained or undrained total stress analysis is carried out to simulate the excavation, hydrostatic pressure distribution around the wall due to lowering of water table within the excavation needs to be incorporated. If these unbalanced forces are ignored, it is inevitable to get lower wall deformations. Ng *et al*. (2004) incorporated these effects in their drained analysis, but they have not discussed in detail the way they incorporated these forces.

In 1992, Hashash proposed a partially coupled analysis based on the principle of effective stress. In this analysis, only the excess pore pressures above the hydrostatic pressures are included. Hence he applied body loads around the wall to take into account the hydrostatic pressure difference on either side of the wall during lowering of the water table inside the excavation.

In this paper, deep excavation simulation within the capabilities of ABAQUS/Standard finite element program is discussed in detail. Three approaches are adopted to obtain the undrained short term behaviour: (i) a fully undrained total stress analysis (ii) a partially-coupled effective stress analysis and (iii) a fully coupled effective stress analysis. The analysis time for the two effective stress analyses is short and selected to avoid any excess pore pressure dissipation during the excavation. Hence both effective stress analyses effectively correspond to the undrained (short term) response during excavation. Undrained and drained soil properties for the total and effective stress analyses, respectively, are derived based on the triaxial test data for the same soil. The partially-coupled analysis used is somewhat similar to the method proposed by Hashash (1992) but application of body loads during the construction stages is different. The main aim of this paper is to investigate the performance of three analysis methods. Hence soil anisotropy or small strain effects are not incorporated in this analysis owing to the large number of empirical parameters involved in those constitutive models, which might hinder the main purpose of this research. First a hypothetical excavation with a support system is analysed using the three analysis procedures. Finally a case study of a staged construction is presented.

2 FINITE ELEMENT MODEL

The multi propped deep excavation was simulated using the ABAQUS/Standard (2010) finite element program assuming plane-strain conditions. This assumption is reasonable for the purpose of this study and when the excavation is fairly long. According to Finno *et al*. (2007), when the excavation length to depth ratio exceeds six, this is a reasonable assumption. However for other instances, where the excavation length to depth ratio is less than six, it should be noted that this assumption will lead to overestimation of the deformations near the corners of the excavation due to the negligence of stiffening effect adjacent to the corners.

Due to the symmetry of the excavation, half of the soil domain is considered. The loading is also assumed to be symmetrical. During the fully and partially coupled effective stress analyses, soil is simulated using eight-node quadratic elements with pore pressure degrees of freedom at the corner nodes. Since the permeability of the wall is negligible compared to the permeability of the soil, the same element without pore pressure degrees of freedom is used to model the slurry wall. Soil and the wall in the total stress analysis are also modelled with the same element without pore pressure degrees of freedom. Mohr-Coulomb model was used to represent the constitutive behaviour of the soil when analysing the hypothetical case. For the case study, Modified Cam Clay (MCC) model is used to represent the soil behaviour, because material model parameters are available only for the MCC model. Simple linearly elastic perfectly plastic model is used to simulate the constitutive behaviour of the concrete wall. The maximum stress level during the analysis is investigated to ensure that the stress level is always below the yield strength of the concrete. Cracking and rebar configurations were not considered for the wall. The analysis neglects the effect of installation of slurry wall and assumes that the wall is "wished in place". This assumption is made merely to avoid convergence issues which could arise due to wall installation. Hence, the initial stresses around the wall before commencement of the excavation is only the geostatic stress state due to overburden stresses and pore pressure distribution is only due to the hydrostatic pressures.

The complicated bracing system is idealized as a rigid support system. The strut locations were restrained from the horizontal movement during the bracing installation step. No further movement of the wall is allowed at the strut locations after the installation of struts. A simple construction sequence is used in the analysis as shown in Figure 1.

Soil elements were removed up to a depth of h_{un} and the first strut is installed at the level of the newly excavated surface. Then the excavation proceeds up to a depth of (h_{un} + h_s) and the second strut is installed at this level. The distance between the ground surface and the water table is h_w. This construction sequence is continued until the excavation depth reaches the critical failure depth for a given wall length. Here the critical failure depth is defined as the depth at which the model stopped running when the soil reaches the critical state strength.

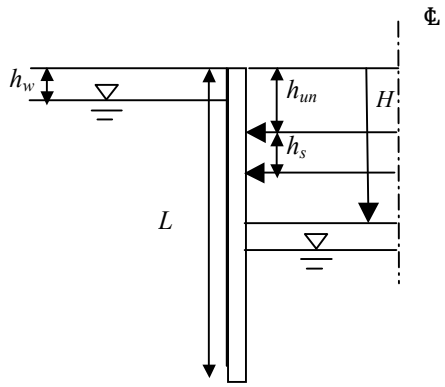

Figure 1: Geometry of the excavation.

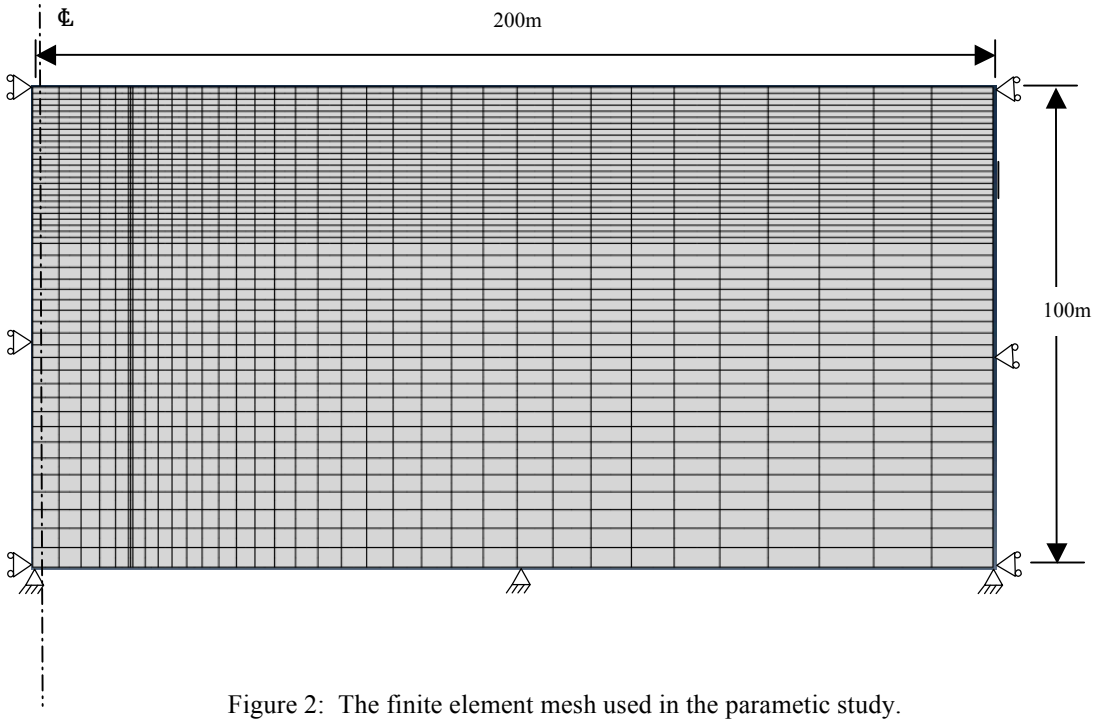

Figure 2: The finite element mesh used in the parametic study.

Regarding the wall-soil interface modelling, Yoo and Lee (2008) discussed the convergence problems associated with the surface based interface algorithm in ABAQUS/Standard (2010). They used a thin layer interface element with six nodes proposed by Desai *et al*. (1984) at the wall-soil interface. Numerical modelling carried out during this study shows that the soil-wall interface behaviour has no significant influence on the ground surface and wall deformations. Hashash and Whittle (1996) also observed the same. Therefore, in this analysis, no slip is allowed at the wall-soil interface. The concrete wall has a Young's modulus of 2.3×10^7 kPa and a Poisson's ratio of 0.2. Table 1 shows the soil properties used for the analysis. These undrained and drained properties are for Boston Blue Clay, and extracted by Hashash (1992) based on triaxial test data. Undrained elastic Young's modulus is calculated by equating the shear modulus for drained and undrained conditions, which is given by:

$$G = \frac{E}{2(1+v)} \tag{1}$$

Table 1: Soil properties used for the analysis, extracted from Hashash (1992)

Soil parameters	**Value**
Total stress analysis	
Undrained shear strength, c_u	0.37 σ'_{vo}
Undrained Elastic Young's modulus, E_u	71 σ'_{vo}
Undrained friction angle, ϕ_u	0
Poisson's ratio (undrained analysis), ν_u	0.495
Earth pressure coefficient at rest, K_o	1.0
Effective stress analysis	
Effective friction angle, ϕ'	33°
Drained Elastic Young's modulus, E'	E_u/1.2
Poisson's ratio (effective stress analysis), ν'	0.27
Earth pressure coefficient at rest, K_o	(1-sinϕ')
Permeability (m/day), k_x, k_y	1.0×10^{-5}
Bulk unit weight of the soil (kN/m^3), γ	18.0

2.1 UNDRAINED ANALYSIS

During the undrained analysis (Case A) soil is considered as a continuum material, following the Mohr-Coulomb failure sat γ_{sat} of the soil. The strains generated during the establishment of initial stress field are assumed to be zero for the subsequent analysis. The lateral thrust acting on the wall due to the hydrostatic pressure is taken into consideration by setting the lateral earth pressure coefficient (K_o) equal to one. The unit K_o condition will apply the lateral pressure due to water and soil on the wall. During soil excavation, water is pumped out of the excavation. Therefore, when the elements are removed to simulate the excavation sequence, the unit K_o condition will automatically remove lateral pressure due to both water and soil over the excavated depth along the wall.

2.2 PARTIALLY COUPLED ANALYSIS WITH BODY LOADS

In this analysis (Case B), hydrostatic forces are considered separately. The coupled consolidation analysis in ABAQUS is based on effective stresses and excess pore pressures, when the body load option is used to apply the soil unit weight to set up the initial effective stress state. Initial equilibrium is established by the body loads applied to the finite element ′)) of the soil and by assigning the initial vertical effective stress distribution and the lateral earth pressure coefficient (K_o). The analysis establishes a zero pore pressure distribution initially and only excess pore pressures above the hydrostatic pore pressures are computed in the subsequent analysis steps.

Normally the wall behaviour is governed by total stresses. Therefore, during the initial step, hydrostatic pressures are applied to the wall as shown in Figure 3(a) because the soil is assumed to be fully saturated and the water table is at the ground surface. During removal of the soil, water is also removed but in the finite element model, soil weight is defined based on the submerged unit weight of the soil. Therefore, an additional load is applied on the excavated surface as shown in Figure 3(b) to simulate the unloading due to water removal. This can be explained mathematically as shown below:

Over the excavated surface: Initial effective stress (Finite element model) $h\gamma'$ (2a)

Reduction in total stress due to soil removal (In reality) $-h(\gamma' + \gamma_w)$ (2b)

Final effective stress (Finite element model) $-h(\gamma' + \gamma_w) + h\gamma' = -h\gamma_w$ (2c)

In addition, the body loads applied on the wall surface on the excavation side should be modified as shown in Figure 3(b) to replicate the removal of water up to the surface of the excavation. The excess pore water pressures are calculated by the finite element code automatically. Hence, the total pore water pressure distribution is given by the addition of externally applied hydrostatic pressures and computed excess pore water pressures. This way of applying external pressures is slightly different to the approach proposed by Hashash (1992), where the water drawdown was simulated by removal of only the top triangular distribution of hydrostatic pressure and leaving the trapezoidal part to replicate the hydrostatic pressures. The latter do not simulate the actual pore pressure distribution and leads to larger pore pressures acting on the excavation side of the wall. Water table within the excavation is kept 2.5 m below the excavated surface to avoid convergence issues. A finite element analysis similar to this is more efficient than a fully coupled effective stress

analysis based on total pore pressures because a partially coupled analysis helps to avoid convergence problems which may arise when advanced soil models are used in a fully coupled analysis dealing with total pore water pressures. This will be discussed in the following section.

2.3 FULLY COUPLED ANALYSIS

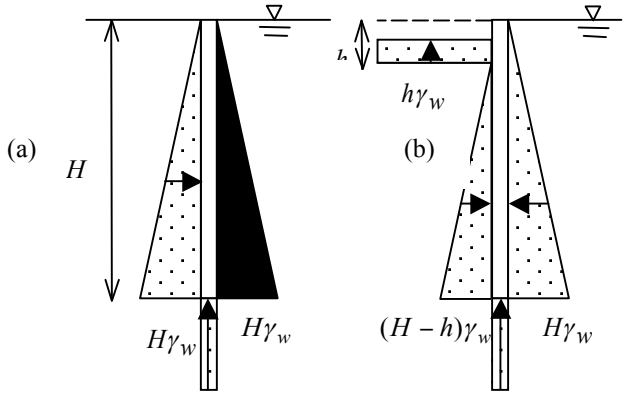

Figure 3: Body forces applied over the wall and excavated surface (Water table is at the ground surface) (a) initial step and (b) during excavation.

In ABAQUS/Standard, a fully coupled analysis (Case C) based on the effective stress principle and total pore pressures will be simulated if the initial stress state is defined using the gravity load option. In the initial step, which establishes the initial stress state within the finite element model, vertical equilibrium of the pore fluid is established using unit weight of the pore fluid and the initial pore pressure distribution applied to the model. The vertical equilibrium of the soil is achieved using the dry unit weight (ρ), initial porosity (n_o), degree of saturation (s) and the initial effective vertical stress distribution (σ'_{zz}) specified for the model. The following equations are used to calculate the initial vertical stress distribution;

$$\frac{d\sigma'_{zz}}{dz} = \rho g - \gamma_w s\left[(1-n_0) - \frac{ds}{dz}\left(z_w^0 - z_0\right)\right] \qquad \text{for} \qquad z < z_1^0 \tag{3a}$$

$$\frac{d\sigma'_{zz}}{dz} = \rho g \qquad \text{for} \qquad z \geq z_1^0 \tag{3b}$$

where z_w^0 is the position of the phreatic surface and z_1^0 is the position of the interface between dry and partially saturated soil. In this case, fully saturated soil with a constant void ratio is considered. If the saturation and the void ratio are a function of depth, Equations 3(a) and (b) need to be integrated to compute the initial stress distribution. Case C is considered as the benchmark when comparing the three cases.

3 COMPARISON OF RESULTS

In this section, results obtained from the three cases given in Section 2 are discussed. The excavation used for the analysis is shown in Figure 1. The excavation is carried out up to a depth of 22.5 m in all cases. For Cases B and C, where excess pore pressure generation and dissipation are incorporated, analysis is carried out within a very short period of time (8.33 m/day) to simulate the behaviour similar to Case A.

The wall height is 40 m and the thickness is 0.9 m. The unsupported height of the excavation, before installation of any struts (h_{un}) is 2.5 m. After excavation of 2.5 m, a strut is installed at the surface level of the excavation. Figure 4 shows the variation of the lateral wall movements with the excavation depth for Case C. This figure clearly shows the initial cantilever deformation after the excavation depth reaches 2.5 m. After each strut installation, wall deformation above installed strut has not been changed due to further excavation. However, the wall starts to bulge below the excavation depth, moving the bottom of the wall towards the excavation. When the excavation depth reaches 22.5 m, the maximum lateral deformation of the wall is about 175 mm.

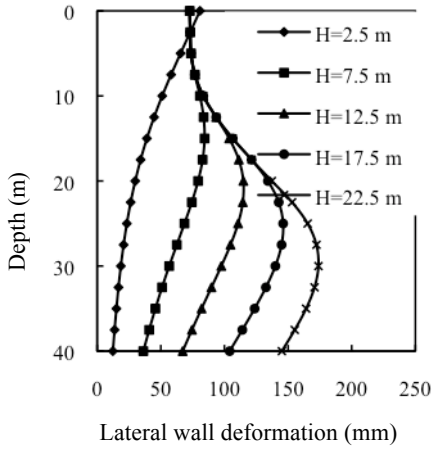

Figure 4:Variation of Lateral wall deformation with excavation depth (*H*).

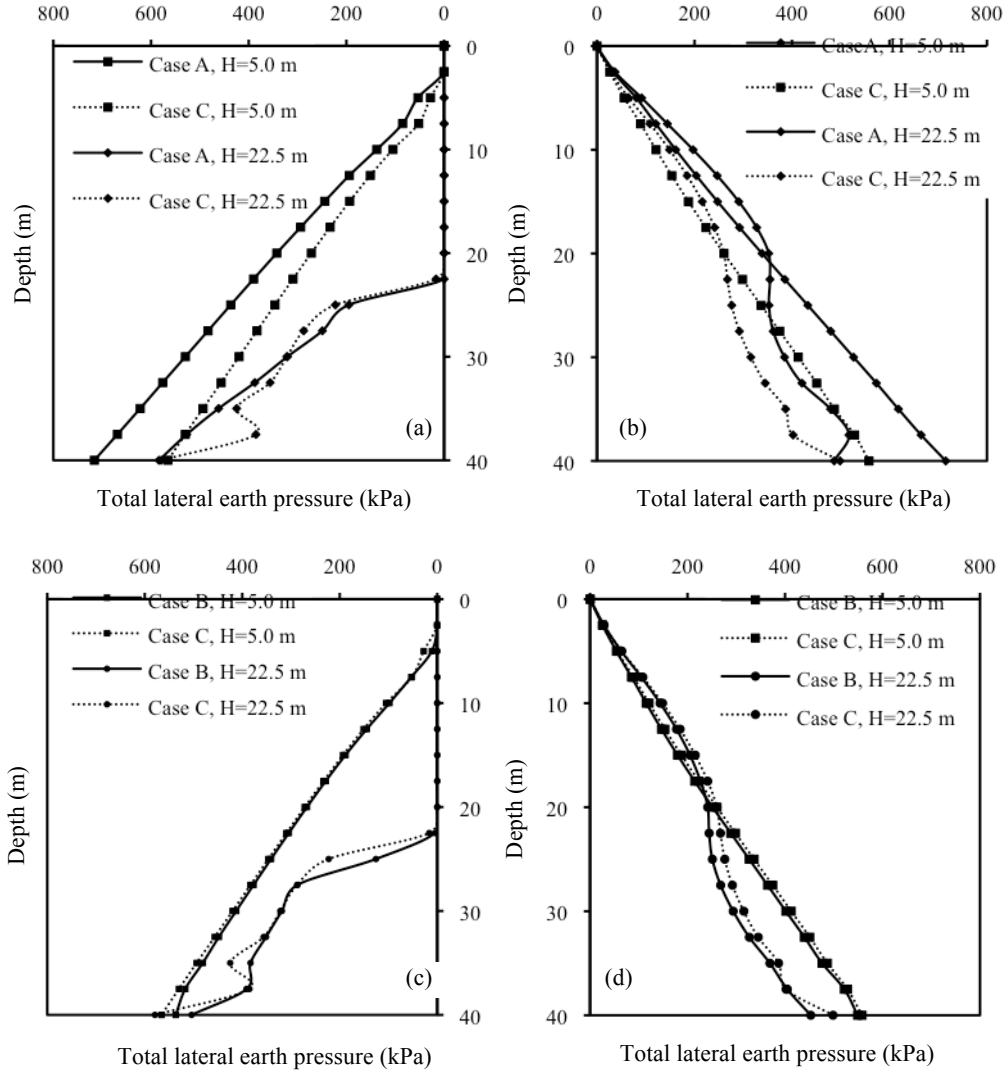

Figure 5. Total lateral earth pressure distribution (a) & (c) excavation side of the wall (b) & (d) behind the wall.

Figures 5(a) to (d) show the distribution of total lateral earth pressures on either side of the wall in accordance with the wall movement, acting at different stages of the excavation for Cases A, B and C. Before the commencement of soil removal, lateral earth pressure distributions behind and in front of the wall are the same. These values are based on the K_o used to establish the initial geostatic stress distribution within the soil and the hydrostatic pressures acting on the

wall in Cases B and C. Due to the lateral movement of the wall towards the excavation, caused by the removal of soil, these pressures will start to change. Since the wall is trying to move towards the excavation, active and passive earth pressure distributions are expected to develop behind and in front of the wall, respectively. However, at shallower excavation depths, there is a substantial difference in the lateral pressure distribution in front of the wall compared to the expected passive pressure distribution in front of the wall.

The earth pressure distribution behind the wall is closer to the expected active earth pressure distribution. This is due to the difference between the initially assigned K_o value, which is 0.45, and the active and passive earth pressure coefficients. The active earth pressure coefficient is 0.37, which is closer to the initial K_o and passive earth pressure coefficient is 2.67. With the increase in excavation depth, earth pressure in front of the wall increases and mobilise the full passive earth pressure. Both Figures 5 (b) and (d) show that the active earth pressures behind the upper part of the wall (over the excavated depth) increase with the installation of struts. Irrespective of the depth of excavation, lateral earth pressures for Cases B and C shown in Figures 5 (c) and (d) agrees well. When the excavation is deeper there is only a small difference in passive pressures predicted for Cases A and C. But the gap between the active pressures is slightly high as shown in figure 5(b) and this will lead to a higher net lateral pressure acting on the wall for the undrained total stress analysis (Case A). Overall these results show that the partially and fully coupled analyses give lateral pressures in agreement but the total stress analysis gives higher lateral earth pressures on either side of the wall compared to Cases B and C.

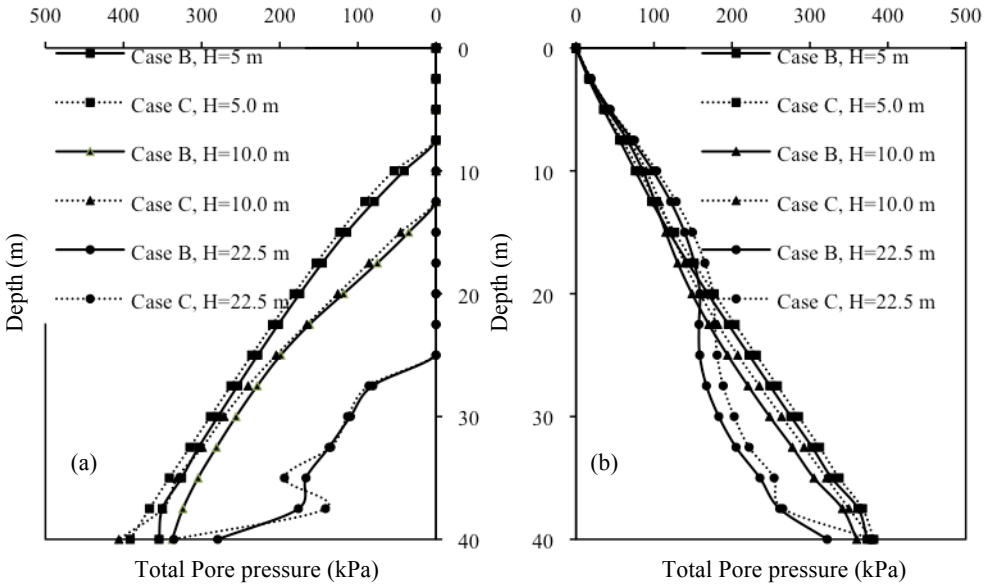

Figure 6. Total pore water pressure distribution on (a) excavation side of the wall (b) behind the wall.

Figures 6 (a) and (b) show the total pore water pressure distribution on either side of the wall for Cases B and C. Figure 6(a) shows the pore water pressures acting on the excavation side of the wall at various stages of the excavation for Cases B and C. Pore water pressure reduction was observed along the centre line of the excavation, below the excavated level due to unloading. When the excavation proceeds, the pore pressure behind the lower part of the wall tends to decrease owing to the stress relaxation caused by the wall movement towards the excavation. Due to the installation of struts, there could be some stress reversals in the points behind the upper part of the wall, which finally results a slight increase in pore pressures. When the excavation depth is shallower, there is only a small difference between the pore pressures acting on both sides of the wall obtained from Cases B and C but this difference tends to increase with the increase in excavation depth. This difference may be due to the decoupling of total pore pressures acting on the wall in Case B into a triangular hydrostatic pore pressure distribution and an excess pore pressure distribution computed by the finite element program.

Figure 7 shows the lateral deformation of the wall for different cases considered, for two stages of the excavation: (i) at the end of the first strut installation after excavation depth of 2.5 m and (ii) at the end of excavation depth of 22.5 m, when h_w = 0. Before installation of any struts, total stress analysis (Case A) matches with the fully coupled analysis (Case C). When H = 2.5 m, partially coupled case (Cases B) slightly over predicts the wall deformations due to the higher pressure deduction on the passive side of the wall during water drawdown.

When the struts are installed with increasing excavation depth, the wall starts to bulge below the excavation depth. Both fully and partially coupled analyses have the ability to take into account pore pressure decrease below the excavation as

a result of stress relief due to excavation. In both total and effective stress analyses, total stresses will also decrease due to soil removal. However, in the effective stress analyses, these reduced pore pressures will increase the effective stresses below the excavation compared to the total stress analysis. These increased effective stresses in the partially and fully coupled analyses will apply higher lateral pressures in front of the wall (Figure 5 (a)) at deeper excavation depths. Hence the bulging of the wall is resisted by moving the wall tip away from the excavation as shown in Figure 7(b).

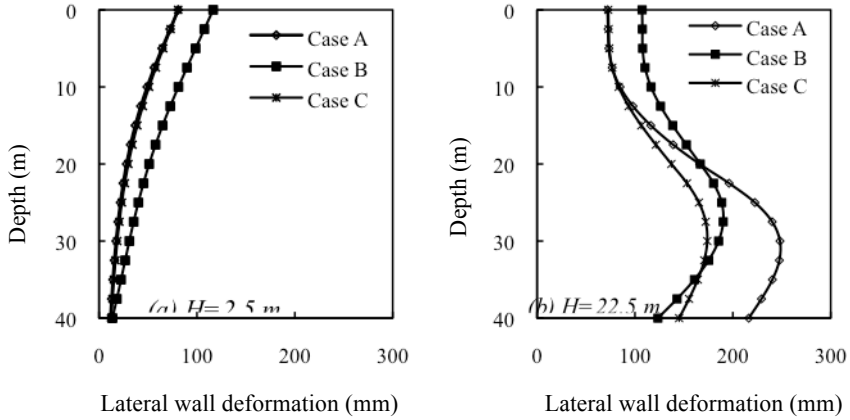

Figure 7. Variation of Lateral wall deformation (a) H=2.5 m (b) H= 22.5 m.

When H = 2.5 m and H = 22.5 m, Case B slightly over predicts the wall deformation compared to Case C. The reason for this slight increase may be due to the application of hydrostatic pressure separately on the wall in the partially coupled analysis (Case B). In the fully coupled analysis (Case C), loads applied on the wall are based on the total pore pressures and effective stresses as in reality, but in Case B, hydrostatic pressure is applied as a separate distributed pressure and the excess pore pressures due to excavation are calculated by the finite element program. Due to decoupling of the total pore pressure acting on the wall, wall deformations of the partially coupled analysis are slightly different to the fully coupled analysis but the total stress analysis over predicts the wall deformations below the excavation.

Figures 8 (a) and (b) show the variation of maximum lateral wall movement and surface settlement of the soil, respectively, with the progression of excavation. The maximum wall deformation obtained from the total stress analysis coincides with that of the fully coupled analysis until the excavation depth is 10 m.

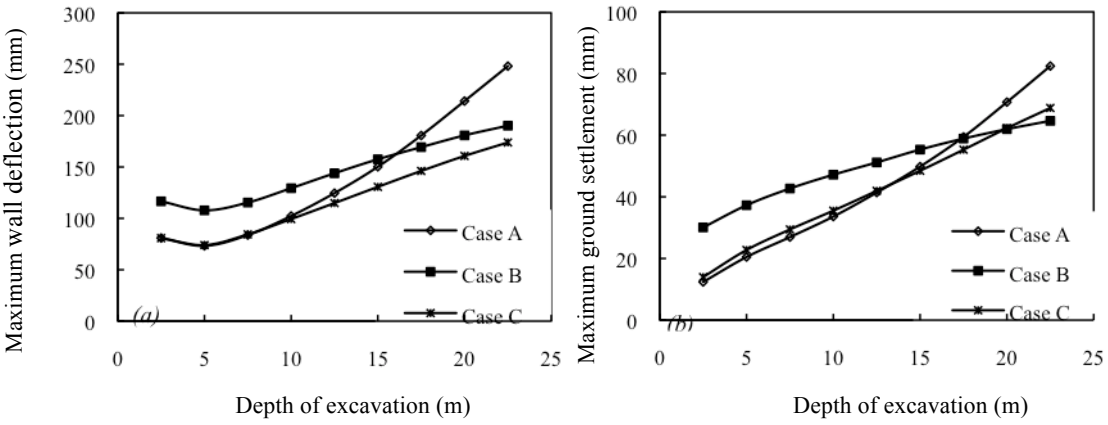

Figure 8. Variation of maximum (a) wall deflection and (b) surface settlement with excavation depth.

Overall, the wall deformations obtained from the partially coupled analysis with separate hydrostatic pressures are higher than that of the fully coupled analysis. This may be due to the decoupling of hydrostatic pressures and excess pore pressures as discussed before. The difference between these results tends to slightly decrease when the excavation depth increases. At deeper excavation depths, total stress analysis produces very high maximum wall lateral deformations as discussed before.

Unlike the wall deformations, maximum ground surface settlement predicted by the total stress analysis is within 20% of the settlement predicted by the fully coupled analysis. Settlements predicted by the partially coupled analysis deviates significantly from the fully coupled analysis. The ground surface settlements behind the wall are governed by the wall deformation. Since wall deformations obtained from the partially coupled analysis are higher than those obtained from the other two cases, predicted settlements are also higher than those obtained from the other two cases. The reason for this is the net lateral earth pressures acting on the wall. As mentioned before, the net lateral force acting on the wall in Case B is higher than Case C and Case A only when the excavation depth is about 10 m. After 10 m, net lateral pressure acting on the wall for Case A increases, increasing wall deformations and ground surface settlements more than those given by other two cases.

Overall, these results show that the undrained total stress analysis is not suitable for the simulation of deep excavations to obtain the short-term behaviour because the total stress analysis tends to over predict the wall lateral deformations and ground surface settlement when the excavation is deep. In addition, total stress analysis does not have the capability to model the water table lowering inside the excavation due to pumping and the effect of water table if it is situated below the ground surface. The lateral earth pressures and pore pressures acting on the wall predicted by partially coupled and fully coupled analyses are in good agreement but the slight variations in net lateral pressures acting over the wall has contributed to higher wall deformations and ground surface settlements from the partially coupled analysis than those predicted by the fully coupled analysis. Therefore, these results conclude that the partially coupled or total stress analysis methods are not suitable for the prediction of short-term behaviour of excavations. In reality, excavations are carried out during a certain period of time in stages while allowing the soil to consolidate. To simulate a construction sequence like that, short-term total stress analysis is not suitable. Therefore, in the following section, performance of the partially and fully coupled analysis methods is further investigated analysing a case study, where a staged excavation is adopted.

4 CASE STUDY

The case study used in this section is the excavation carried out for the hong-hsi garden field building at Hsin-yih Road, Taipei, Taiwan and is surrounded by many buildings. The basement of the building occupies a plan area of 3812 m^2. An intensive monitoring system was used to observe the changes throughout the excavation in the surrounding soil domain. Two bore holes were used to investigate the soil and ground water conditions. The soil at the site is mainly dominated by silty clay up to the depth of 50 m and weathered rock was identified below that level. Laboratory tests were carried out using soil samples obtained at various depths. Four major stratigraphic layers were identified based on an average soil profile. Soil parameters are summarized in Table 2 (Hsi and Small, 1993). Soil in the Taipei basin was found to be highly over consolidated at shallower depths.

Table 2: Soil properties used for the case study.

Layer No	Elevation (*m*) (Levels based on Figure 11)	Unit weight *(kN/m^3)*	Lateral earth pressure coefficient	Permeability $k_x.k_y$ *(m/day)*	Void ratio	Cam Clay parameters		
						M	λ	κ
1	+10.0 to -1.0	18.4	0.43	0.1	1.008	1.16	0.150	0.015
2	-1.0 to -12.0	18.0	0.52	0.05	1.129	1.04	0.160	0.017
3	-12.0 to -22.0	17.9	0.45	0.05	1.127	1.20	0.180	0.013
4	-22.0 to -40.0	20.7	0.47	1.0	0.574	1.17	0.090	0.008

Variation of OCR values for the Taipei basin with depth given by Woo and Moh (1990) is shown in figure 9. Overconsoldation ratio was simulated by varying the pre-consolidation pressure with respect to depth. Ground water table was found 1 m below the ground surface before the excavation and the position of the water table was monitored during the excavation. Pore pressure distribution was found to be hydrostatic up to 14 m but below that depth pore water pressure was slightly less than the static pore water pressure. Prior to the excavation, a 13 m deep perimeter slurry wall with a thickness of 0.6 m was constructed as a permanent retaining structure and bored piles were installed to support the building loading. Excavation was started on July 13 and continued until 7 September of the same year. Whilst the excavation was carried out, the retaining wall was temporarily braced by H beams at four levels as illustrated in figure 10. in the finite element model, the struts weremodelled using one node spring elements. Figure 11 shows the construction sequence used for the analysis including the strut locations.

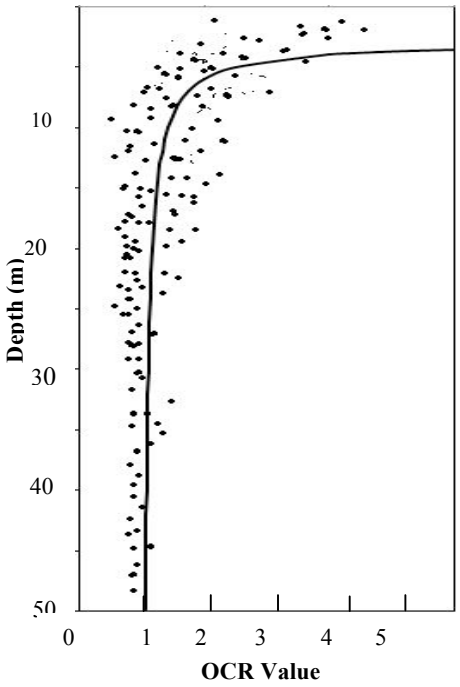

Figure 9: Variation of OCR with depth

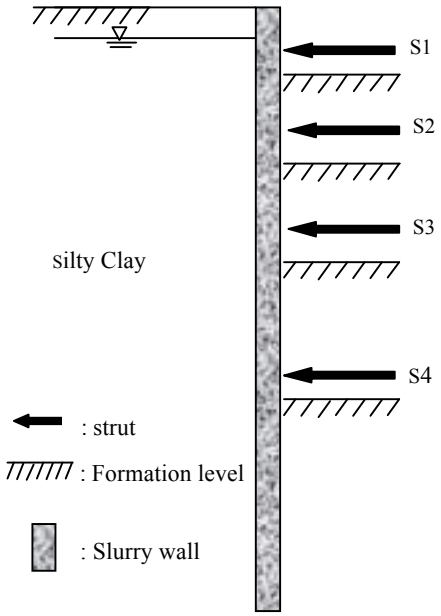

Figure 10: Cross Section of the excavation

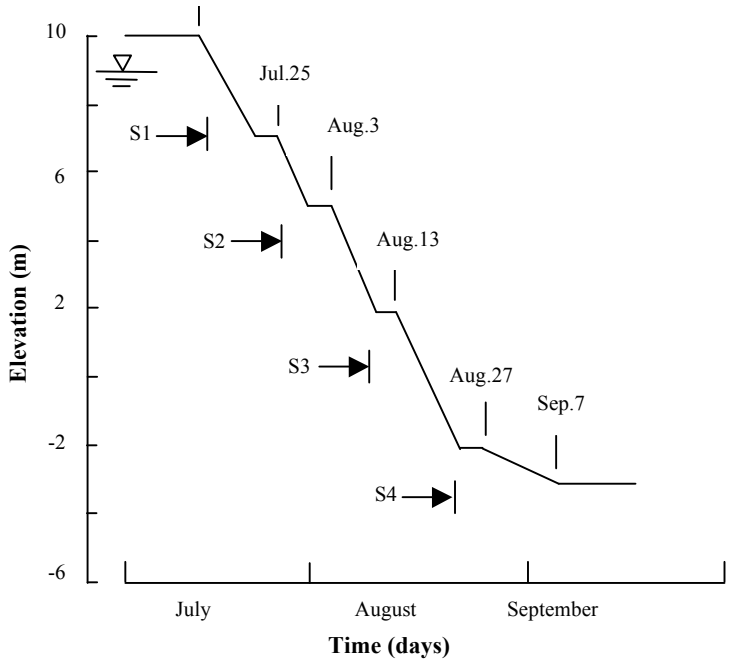

Figure 11. Construction sequence

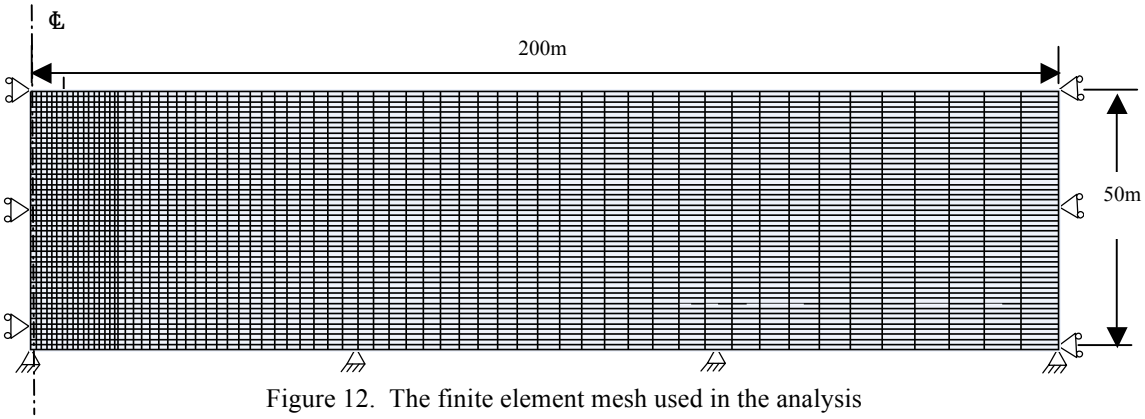

Figure 12. The finite element mesh used in the analysis

The finite element mesh used for the analysis is shown in Figure 12. Ignoring the corner effects, a mid-section is modelled assuming plane-strain conditions. Wall is modelled as an impermeable elastic material with Young's modulus of 2.1x107 kPa and Poisson's ratio of 0.1 using eight-node elements without pore pressure degrees of freedom. Soil is modelled using the same element but with pore pressure degrees of freedom at the corner nodes. Excavation is simulated using both effective stress based analysis techniques discussed in the previous section (partially and fully coupled). A fully undrained total stress analysis is not performed here as it does not have the ability to model the water table, when it is below the ground surface as in this case. In addition, this case study results are given at different stages of the excavation which incorporates consolidation effects.

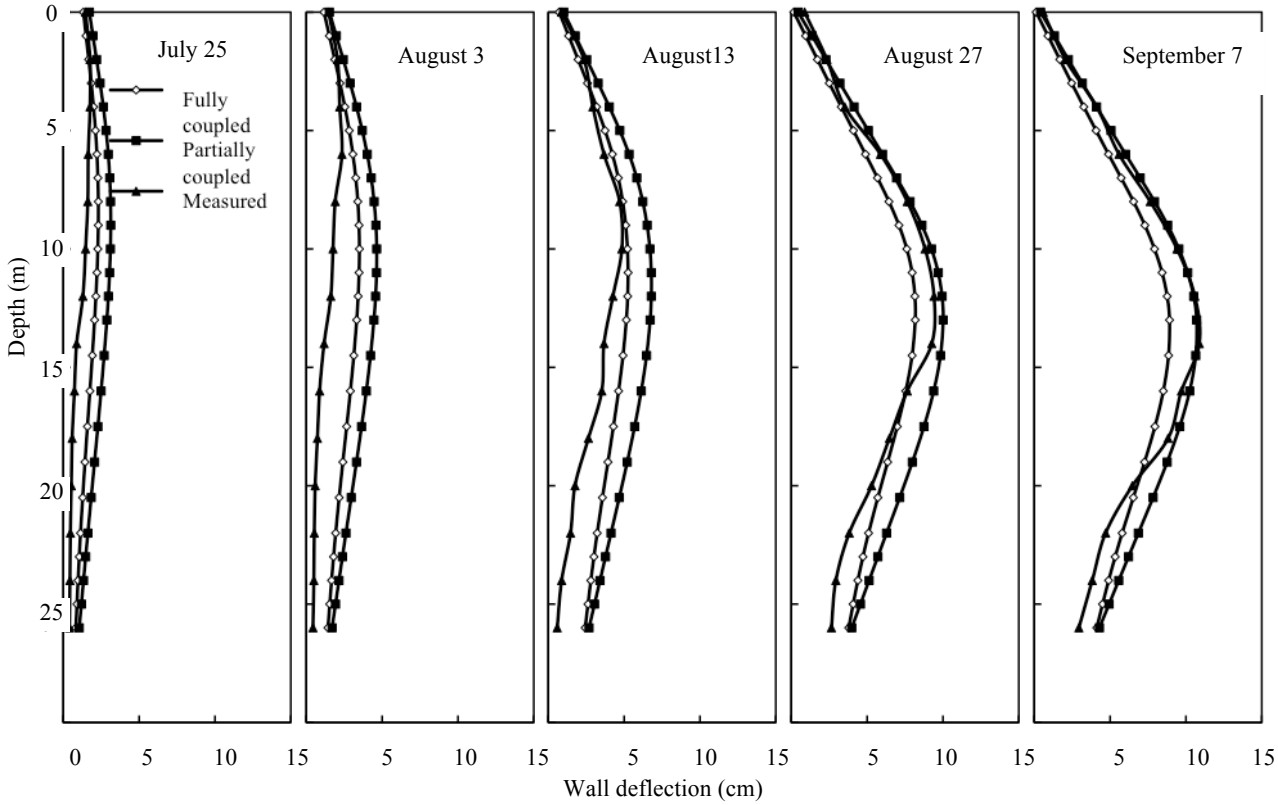

Figure 13. Wall deflection.

The field measurements and computed results from the finite element model using partially and fully coupled analyses are compared and evaluated in this section. Figure 13 shows the computed and measured wall deformations at the end of each main construction stage illustrated in Figure 11. The results from the fully coupled effective stress analysis agrees well with the measured data at the initial four stages but at the final stage, wall deformations are under predicted. The results from the partially coupled analysis over predicts the lateral deformations at the initial four stages but at the

final stage agrees well with the measured wall deformation. The difference between lateral wall deformations obtained from the partially coupled analysis and fully coupled analysis is less than 20% at all five stages. Therefore it can be concluded that both analysis methods based on the effective stress principle are suitable for the simulation of staged excavations, when the consolidation of soil is incorporated.

5 CONCLUSIONS

This paper has investigated three different approaches available in ABAQUS/Standard to simulate the excavations under undrained condition based on total and effective stress principles. The fully coupled analysis is considered as the benchmark and results from other two cases are compared with it. Results show that the conventional way of analysing an excavation using undrained soil properties based on the total stress principle over predicts wall deformations and ground settlements when the excavation depth exceeds about 10 m but for shallower excavation depths conventional total stress analysis agrees well with the fully coupled analysis. The partially coupled analysis over predicts both wall deformations and ground surface settlements compared to the fully coupled analysis because of the decoupling of excess pore pressures and hydrostatic pore pressures along the wall surface. Therefore, it can be concluded that to capture the undrained behaviour of the wall deformation and ground deformations, fully coupled analysis is essential.

Finally, the two analysis methods based on the effective stress principle are applied to a case study of a staged excavation where excess pore pressure dissipation is allowed during the excavation. It was found that the fully coupled analysis agrees well with the measured data during the staged excavation except at the last stage. Partially coupled analysis agreed well with the measured data only at the last stage but in previous stages, it over predicts the wall deformations. However, during all stages, the difference between partially and fully coupled analyses is less than 20%. Hence we can conclude that when the excess pore pressure dissipation is allowed (partially drained), both analysis methods based on the effective stress principle is acceptable to obtain wall and soil deformations during excavations.

6 ACKNOWLEDGEMENT

The authors would like to acknowledge the financial assistance provided by the Australian Research Council for this research under the Discovery grant DP1094309.

7 REFERENCES

ABAQUS Inc.(2010), *ABAQUS version 6.10 user's manual*, Providence, Rhode Island, USA.

Andresen L (2006), *"Parametric FE study of loads and displacements of braced excavations in soft clay,"* Sixth European Conference on Numerical Methods in Geotechnical Engineering ,Graz, Austria, pp. 399-403.

Costa PA, Borges JL and Fernandes MM (2007), "*Analysis of A Braced Excavation In Soft Soils Considering the Consolidation Effect,*" Geotechnical and Geological Engineering, vol. 25, pp. 617–629

Desai CS, Zaman MM, Lightner JG and Siriwardance HJ (1984), "*Thin-layer elements for interfaces and joints*," International Journal for Numerical and Analytical Methods in Geomechanics, vol. 8(1), pp. 19–43.

Finno RJ and Harahap IS (1991), "*Finite element analysis of HDR-4 excavation,*" Journal of Geotechnical & Geoenvironmental Engineering, ASCE, vol. 117(10), pp. 1590-1609.

Finno RJ, Blackburn JT and Roboski JF (2007), *"Three-dimensional effects for supported excavations in clay,"* Journal of Geotechnical & Geoenvironmental Engineering, ASCE, vol. 133 (1), pp. 30–36.

Hashash YMA (1992), *"Analysis of deep excavations in clay,"* PhD thesis, Dept. of Civ. Engrg., Massachusetts Inst. of Technol. (MIT), Cambridge, Mass.

Hashash YMA and Whittle AJ (1996), "Ground movement prediction for deep excavations in soft clay", Journal of Geotechnical Engineering, ASCE, vol. 122(6), pp. 474–486.

Hou YM, Wang JH and Zhang LL (2009), *"Finite-element modeling of a complex deep excavation in Shanghai,"* Acta Geotechnica , vol. 4, pp. 7–16.

Hsi JP and Small JC (1993), *"Application of a fully coupled method to the analysis of an excavation,*" Soils and Foundations, Japanese Society of Soil Mechanics and Foundation Engineering, vol. 33(4), pp. 36-48.

Hsieh PG and Ou CY (1998), *"Shape of ground surface settlement profiles caused by excavation,*" Canadian Geotechnical Journal, vol. 35(6), pp. 1004-1017.

Hu ZF, Yue ZQ, Zhou J and Tham LG (2003), *"Design and construction of a deep excavation in soft soils adjacent to the Shanghai Metro tunnels,"* Canadian Geotechnical Journal, vol. 40(5), pp. 933-948.

Karlsrud K and Andresen L (2005), *"Loads on braced excavations in soft clay,"* International Journal of Geomechanics, ASCE, vol. 5(2), pp. 107-113.

Kumar J and Chakraborty D (2012), *"Stability numbers for an unsupported vertical circular excavation in c–ϕ soil,"* Computers and Geotechnics, vol. 39, pp. 79–84.

Khatri VN and Kumar J (2010), *"Stability of an unsupported vertical circular excavation in clays under undrained condition.*" Computers and Geotechnics, vol. 37, pp. 419–424.

Kung GTC, Hsiao ECL and Juang CH (2007), *"Evaluation of a simplified small-strain soil model foranalysis of excavation-induced movements,"* Canadian Geotechnical Journal, vol 44 (6), pp. 726–736.

Ng CWW, Simpson B, Lings ML and Nash DFT (1998), *"Numerical analysis of a muti-propped excavation in stiff clay,"* Canadian Geotechnical Journal, vol. 35, pp. 115-130.

Ng CWW, Leung EHY, Lau CK (2004), *"Inherent anisotropic stiffness of weathered geomaterial and its influence on ground deformations around deep excavations,''* Canadian Geotechnical Journal, vol. 41(1), pp. 12-24.

Ou CY, Hsieh PG and Chiou DC (1993), *"Characteristics of ground surface settlement during excavation,"* Canadian Geotechnical Journal, vol. 30, pp. 758-767.

Tang YG and Kung GTC (2010), *"Investigating the effect of soil models on deformations caused by braced excavations through an inverse-analysis technique,"* Computers and Geotechnics, vol. 37(6), pp. 769-780.

Woo SM and Moh ZC (1990), *"Geotechnical Characteristics of Soils in the Taipei Basin,"* Proceedings, 10th South Asian Geotechnical Conference, Taipei, vol. 2, pp. 51-65.

Yoo C and Lee D (2008), *"Deep Excavation-induced Ground Surface movement Characterstics - A numerical Investigation,"* Computers and Geotechnics, vol. 35, pp. 231-252.

Zdravkovic L, Potts DM and St John HD (2005), *"Modelling of a 3D excavation in finite element analysis,"*, Geotechnique, vol 55(7), pp. 497-513.

List of symbols

h_{un} – Unsupported depth of excavation
h_s – Vertical spacing
h_w – Depth of water table
L – Length of wall
H – Depth of the excavation
c_u – Undrained shear strength
E_u – Undrained Elastic Young's modulus
ϕ_u – Undrained friction angle
v_u – Poisson's ratio (undrained analysis)
K_o – Earth pressure coefficient at rest
ϕ' – Effective friction angle
E' – Drained Elastic Young's modulus
v' – Poisson's ratio (effective stress analysis)
k_x, k_y – Permeability
σ'_{vo} –Vertical effective stress
G – Shear modulus
γ_{sat} – Saturated unit weight
′) – Submerged unit weight
γ_w – Unit weight of water
ρ – Dry density
n_o –Degree of saturation
σ'_{zz} –Vertical effective stress
g – Gravitational acceleration
z – Vertical coordinate
z_w^0 – Position of the phreatic surface
z_1^0 – Position of the interface between dry and partially saturated soil
M –Slope of the Critical state line
λ –Slope of the normal compression line
κ –Slope of swelling line